Techniques Towards Understanding Shear Dependent Thrombus Formation

I. Pinar[1,2], J. Arthur[3], R. Andrews[3], E. Gardiner[3], K. Ryan[1] and J. Carberry[1,2]

[1]Department of Mechanical and Aerospace Engineering
Monash University, Victoria, 3800, Australia

[2] Division of Biological Engineering, Faculty of Engineering
Monash University, Victoria, 3800, Australia

[3] Australian Centre for Blood Diseases,
Monash University, Victoria, 3800, Australia

Abstract

Several novel techniques are presented to provide both a qualitative and quantitative method of analysing shear dependent thrombus growth in real-time. Thrombus geometries are grown (*in vitro)* and imaged through four-dimensional (4D) confocal microscopy. Techniques to reconstruct a time corrected stack of confocal images into a three-dimensional (3D) surface are presented. The flow of blood (*in silico*) over the thrombus geometry is modelled by attaining a solution to the incompressible and steady state Navier-Stokes equations through the OpenFOAM package. Previous work [5] has shown thrombus growth and platelet activation is highly sensitive to shear. As such the methods presented allow for the shear forces which platelets undergo prior to adhesion to be correlated with a range of parameters, including growth. The combination of these techniques allow for highly temporally and spatially resolved comparisons to be made as to the underlying mechanisms of platelet adhesion and aggregation.

Introduction

Platelets are a crucial component in thrombus (blood clot) formation and the prevention of major blood loss after vascular injury. The mechanisms driving platelet aggregation into consolidated thrombi are not sufficiently understood to improve anti-platelet therapies. Current knowledge in this field has for a long time focused on the biochemical interactions responsible for initiating thrombus growth but more recently the role of flow induced shear forces has been investigated [7]. Platelets are highly sensitive towards changes in the shear stresses within a blood vessel and variations in shear alone can promote platelet adhesion and aggregation in the absence of other biochemical stimulus. The precise mechanisms responsible for shear induced platelet adhesion and aggregation remain poorly understood.

In the current work the flow dynamics around experimentally grown thrombus geometries is examined in a detailed numerical (*in silico*) and experimental (*in vitro*) setting. A set of unique techniques to analyse thrombus growth and retraction with high temporal and spatial resolution is introduced. These techniques allow for thrombus formation characteristics to be quantified from an entire thrombus field (300 μm scale) with individual platelet level resolution (2 μm scale). Such quantifications enable direct comparisons between the growth of a thrombus based on a certain Lagrangian shear time history of individual platelets.

Methodology

Experimental Flow Loop

Human whole blood (1) was uniformly stained with membrane-permeable fluorescent dye $DiOC_6$ to visualise platelets, and was pulled through a 0.2mm × 2.0mm collagen coated glass micro channel for 3 minutes by a Harvard Syringe Pump (4) at 1.44 ml.min^{-1} generating a wall shear rate (γ_w) of 1800 s^{-1}. Platelets adhere and form aggregates of 10-60 μm in height within 1-3 minutes after exposure of flowing blood to collagen. The flow profile was measured through an inline flow probe (2) and recorded. Thrombus aggregations were imaged using an immunofluorescence confocal microscope (Nikon, A1) in real-time using 0.7 μm thick slices with a pixel density of 0.63 μm/pixel.
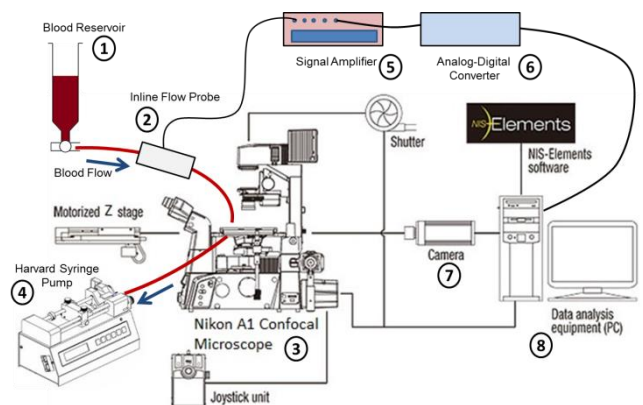

Figure 1. Schematic of the flow loop used for the *in vitro* experiments. Blood was pulled from the reservoir (1) through the micro channel by the syringe pump (4). Flow profile was measured via the inline flow probe (2). A confocal microscope (3) images real-time thrombus growth for the 3 minutes of blood flow.

Segmentation

The slices acquired from the confocal microscope are stacked vertically and converted from 12-bit to 8-bit to apply a greyscale spectrum threshold based on pixel intensity. In-house segmentation software was then used to isolate individual thrombus boundaries. Individual boundaries are combined vertically to generate a three-dimensional (3D) point cloud and a 3D surface is fitted enclosing the point cloud using Avizo [4].
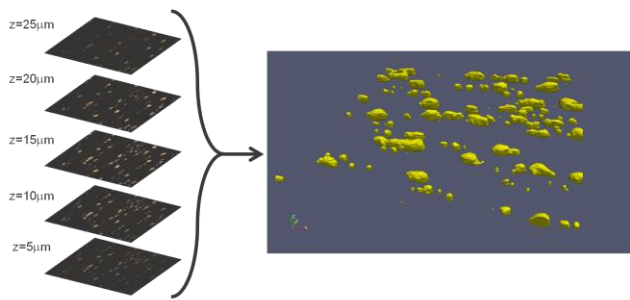
Figure 2. Thrombus reconstructions consist of the individual 2D confocal image slices being stacked on top of each other (left). Individual thrombi thresholds are established across all slices to form a 3D point cloud. A 3D surface is fitted to these points to generate the surface in yellow (right).

Time-Corrected Thrombus Field Generation

Using a slice thickness of 0.7 μm, the confocal microscope acquires an image z-stack, scanning vertically through a typical sized thrombus (75μm (L) × 12μm (W) × 42 μm (H)), in approximately 3.5 seconds. A major consideration is that the thrombus continuously grows during the time it takes to image the z-stack. In order to study changes in thrombus geometries between z-stacks we must therefore correct for the changes that occur during the acquisition of the z-stack. A solution to this issue, which allows for a time-corrected thrombus stack, is to morphologically generate the intermediate confocal slices at each z-level as demonstrated in Figure 3. This is accomplished by utilizing a modified active contour level set method which treats the minima as the enclosing bounds around a particular thrombus between two points in time [2]. The initializing contour is defined by the boundary around the thrombus for a particular slice in the initial time stack. The resulting curves are evolved over time to produce the confocal slices between two time points. Every intermediate slice is then assigned a real-time value which is synchronized with the camera shutter timing from the confocal microscope to give time-corrected slices of the thrombus at any

point in time. In addition to this, there is a time delay introduced by the piezo-z stage used on the microscope which occurs during the movement of the stage from the top of the thrombus to the bottom. The algorithm accounts for this time difference in the time-corrected slices by using the recorded position of the stage in z with respect to time and correspondingly assigns the correct real-time to any particular slice.

A limitation to this technique is the reduction of the number of acquired stacks by two and therefore the reduction of the total measurable time by 3.5 seconds. This is due to the level set method requiring two individual images to be able to perform the curve evolution step. Time-corrected slices cannot be generated for times prior to the time at the end of the first stack and also times after the beginning of the last stack. Figure 3 shows this limitation in more detail, for which time-corrected slices cannot be created for times less than 3.5 seconds or greater than 4 seconds. While only two real-time acquired confocal stacks are shown for clarity, there is no limitation on the number of image stacks the technique is capable of handling.

Thrombus Growth Calculation

The ability to determine the real-time spatial location and volumetric growth of a thrombus is of particular significance when investigating and establishing the underlying mechanisms which drive thrombus formation. Thrombus growth is calculated as the spatial distance between two points in time. The surface normals from the initial time point are projected both outwards and inwards so as to intersect with the surface at the final time point. Constructing multiple surface normal rays is necessary to ensure both growth and retraction of the thrombus are accounted for. The corresponding distances are then mapped onto the initial surface shown in Figure 4, where red indicates regions of thrombus growth, while blue represents thrombus retraction or thrombus reduction through embolism.
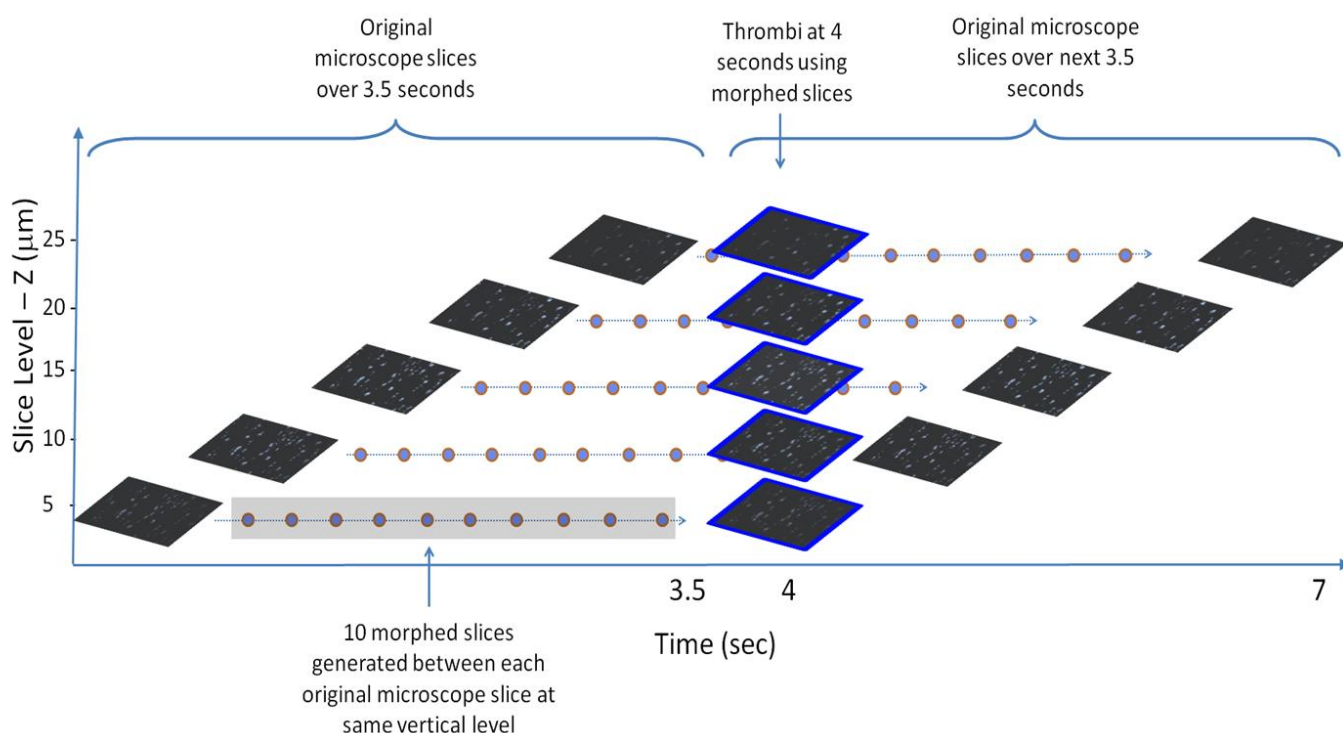

Figure 3. Illustration of two typical stacks of images with the corresponding time-corrected image stack. Slices between t=0-3.5 seconds and t=4-7 seconds represent real-time images captured using the confocal microscope. A total of 10 intermediate slices are generated between any 2 slices at a particular level in Z. The slices highlighted in blue represent the resulting slices generated for the thrombus stack at t=4 seconds.
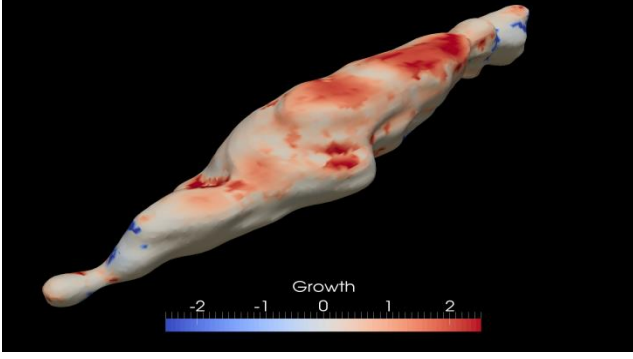
Figure 4. Representation of thrombus growth over a one second period. Red indicates regions of growth while blue represents retraction/loss.

Numerical Technique

Flow through the numerical domain was steady as measured through the flow probe, with blood being considered as an incompressible and Newtonian fluid. The numerical model maintains the same Reynolds number (Re) as the experimental flow with Re $\approx$ 4.2 (based on channel height). The model preserves the same aspect ratio (AR) where:

$$AR = \frac{W}{H} \qquad (1)$$

where W and H are the width and height of the channel respectively. The length of the channel is reduced in the model from the experimental micro channel length of 100mm to 60mm to decrease the computational resources required. A solution to the incompressible Navier-Stokes equations to steady state is attained through the OpenFOAM ® solver package utilising the SIMPLE algorithm [1].

The numerical domain consists of a channel with the thrombus geometry located at the center of the channel. Figure 5a) illustrates the configuration of the numerical domain which consists of several different boundaries. The inlet to the micro channel has a fully developed parabolic velocity profile with a mean velocity of 0.06 ms^{-1} (corresponding to γ_w = 1800 s^{-1}) in combination with a Neumann pressure boundary. The outlet has a zero pressure Dirchelet boundary and a Neumann boundary for velocity. The top, bottom and sides of micro channel and the thrombus surface all have a zero velocity Dirichlet boundary condition imposed. A polyhedral finite volume mesh is utilised throughout the domain with a refinement region 200 μm radially around the thrombus geometry. Figure 5b) is an example of a typical domain mesh consisting of approximately 9 million elements, with the thrombus surface accounting for around 8.4 million of these elements. A surface grid resolution study was performed with the error being below 0.1%. The numerical domain was solved to a steady state with velocity and pressure residuals being less than 10^{-10}.

The local shear rate is calculated using,

$$\gamma_{local} = \sqrt{2 \times D{:}D} \qquad (2)$$

where D is the strain rate tensor with U the velocity vector field,

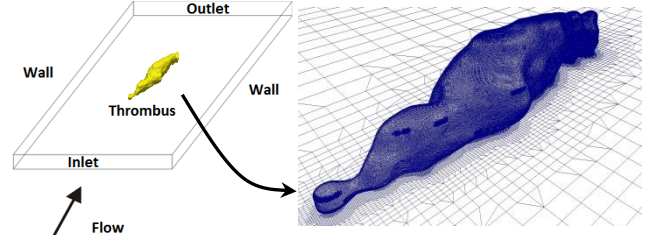$$D = \nabla U + (\nabla U)^T \qquad (3)$$

Figure 5. a) Diagram of the numerical domain with the thrombus located at the center of the channel. b) Representation of a typical thrombus after surface and refinement region meshing

Shear Correlation

The combination of shear and the corresponding growth provides a powerful tool for understanding the mechanisms which govern platelet adhesion under various hemodynamic conditions. The solution to the *in silico* flow field is used to determine the shear forces individual platelets experience throughout the thrombus interaction region (TIR) culminating in interaction with the thrombus surface where the platelet may, or may not, adhere. The TIR is defined as a distance that is upstream 10% of the overall thrombus length in the direction of flow and provides an indication as to where the platelet begins to experience shear gradients that are directly caused by the thrombus geometry. For every point on the thrombus surface (approximately 27, 000 points for a typical thrombus) a path line is calculated backwards in time. The path lines are generated by integrating the velocity vector field in the upstream direction from the starting point on the surface. A fourth-order adaptive Runge-Kutta method is implemented and used to integrate the velocity field to determine the spatial path taken by a platelet and the corresponding shear rates at each point along this path line [6]. The error along the path line is maintained below 10^{-8}. However as the thrombus surface has a Dirichlet boundary condition imposed the path lines cannot start from the points along the surface (U$_{surface}$ = 0 ms^{-1}). Consequently each surface point is displaced 1μm (~ platelet radius) in the direction of the surface normal. This not only allows for the path lines to be generated but also is indicative of the location of the centre of the platelet when it makes contact with the surface. Pertinent properties along these path lines, demonstrating the hemodynamic forces a platelet experiences prior to adhesion, are then mapped onto the thrombus surface.
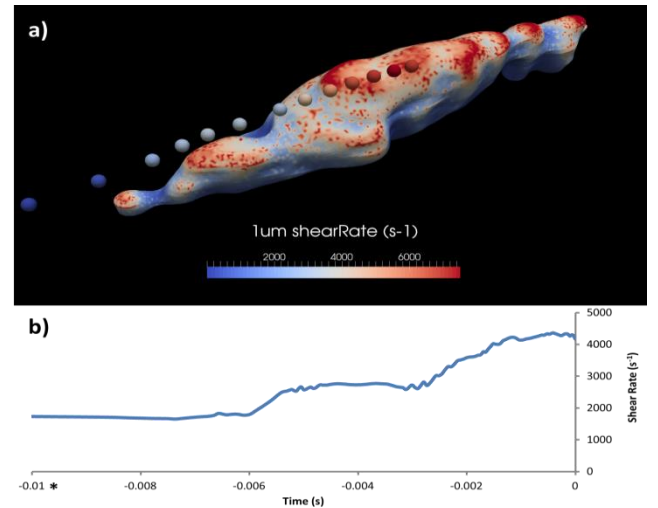

Figure 6. a) Shear rate (s^{-1}) at 1μm above the surface. The spheres represent the path taken by an individual platelet coloured by shear rate (s^{-1}). b) The change in shear rate along the path line with respect to time. * Note: Total time for platelet to reach TIR is 0.23 seconds however only points representing the last 0.01 seconds prior to adhesion are shown.

The use of CFD to determine the flow fields provides the key advantage of being able to extract the Lagrangian description of the flow and therefore determine the time varying shear stresses experienced by individual platelets in the flow field. Moreover, the shear stress experienced by platelets approaching growing thrombi and the shear at the thrombus surface was determined across the entire thrombus field. Reconstruction of the 3D thrombus fields also provides quantification of thrombus growth rates. Figure 6 demonstrates the shear forces experienced by an incoming platelet into a region of high shear on the thrombus surface. The peak shear experienced by a platelet in the vicinity of a thrombus geometry is significantly higher than the wall shear rate which agrees with past studies [1]. Figure 6b) represents the Lagrangian shear history of an individual platelet in the last 0.01 seconds before adhesion. Over a period of 0.006 seconds the platelet experiences an increase over the wall shear rate of 133%. Such large shear gradients are thought to trigger platelet activation as shown in a previous study [5] probably by shear-enhanced activation of platelet adhesion receptors such as glycoprotein Ib-IX-V complex to bind collagen and other plasma proteins such as von Willebrand factor.
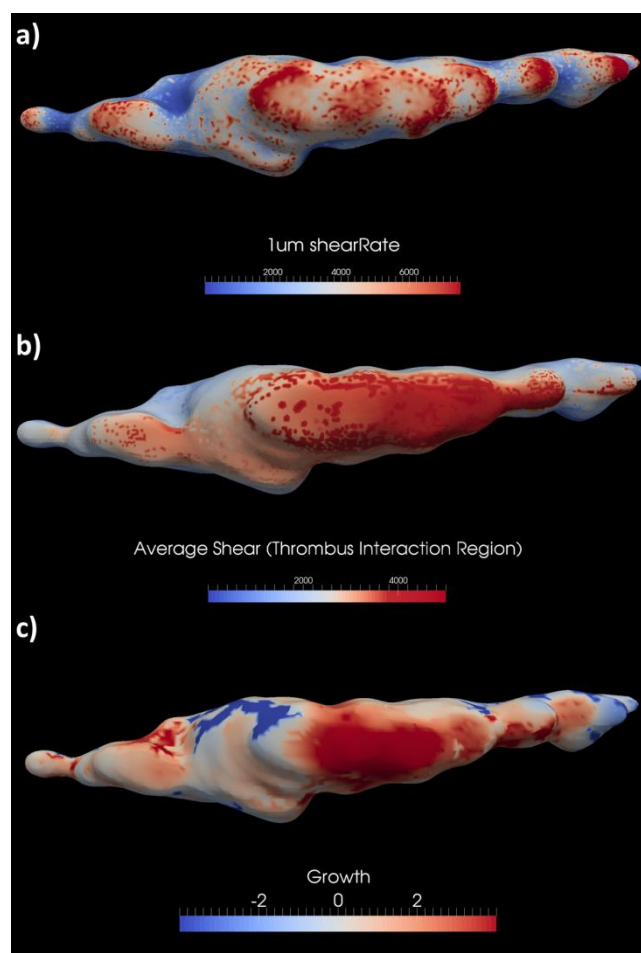

Figure 7. a) Shear rate 1 μm above the thrombus surface b) Represents the average shear rate experienced along every platelets path, respectively, within the TIR that adheres to a point on the surface. c) Regions of growth and loss averaged over 10 seconds shown on the growing surface.

Figure 7 (a-c) illustrates key properties of platelets moving through the flow field prior to adhesion and these can be compared to the subsequent thrombus growth, Figure 7c). The shear rate 1 μm above the surface is indicative of the shear platelets experience at the point of adhesion, Figure 7a). The

average shear along an individual platelets path up to the point of adhesion, Figure 6b), reveals that shear at the thrombus surface is not the only indicator of favourable regions for platelets to adhere. Averaged thrombus growth over 10 seconds, Figure 7 c), is comparable to the average shear platelets in these growth regions experience. The area under the shear profile along the platelets path shows regions of high shear area which will aid definition of the shear contribution to thrombus formation.

Conclusions

We present a novel combination of *in-vitro* and *in-silico* experiments to investigate platelet adhesion and thrombus formation. We demonstrate the real-time reconstruction of time corrected stacks of confocal images of a growing thrombus. Correlation of the shear experienced by individual platelets prior to interacting with the thrombus surface with the observed subsequent thrombus growth provides a powerful analysis tool towards understanding the shear dependence of thrombus formation.

Acknowledgments

References

[1] Butler, C., Ryan, K. & Sheard, G., Haemodynamic forces on in vitro thrombi: a numerical analysis, *Med. Biol. Eng. Comput.*, **50**, 2012, 493-50

[2] Chan, T.F. and Vese, L.A., Active Contours Without Edges, *IEEE Trans. Image Proc.*, **10**, 2001, 266-77

[3] OpenFOAM ® open source computational fluid dynamics (CFD) toolbox, *ESI-OpenCFD*, Version 2.1.1, 2014, http://www.openfoam.com

[4] Avizo ® Standard 3D Analysis Software for Scientific Visualization, *FEI™ Visualization Sciences Group (VSG)*, Version 8.1.0, 2014 http://www.vsg3d.com/avizo

[5] Nesbitt, W.S., Westein, E., Tovar-Lopez, F.J., Tolouei, E., Mitchell, A., Fu, J., Carberry, J., Fouras, A. & Jackson, S.P., A shear gradient-dependent platelet aggregation mechanism drives thrombus formation, *Nat. Med.*, **15**, 2009, 665-673

[6] Press, W.H., Flannery, B.P., Teukolsky, S.A. & Vetterling, W.T., Numerical Recipes: The Art of Scientific Computing, *Cambridge University Press*, **3**, 2007, 907-20

[7] Tolouei, E., Butler, C.J., Fouras, A., Ryan, K., Sheard, G.J. & Carberry, J., Effect of hemodynamic forces on platelet aggregation geometry, *Ann Biomed Eng.*, **39**, 2011, 1403-1413